energies

MDPI

Article

# ZnS/$SiO_2$ Passivation Layer for High-Performance of $TiO_2$/$CuInS_2$ Quantum Dot Sensitized Solar Cells

**Hee-Je Kim [1], Jin-Ho Bae [1], Hyunwoong Seo [2], Masaharu Shiratani [3] and Chandu Venkata Veera Muralee Gopi [1,*]**

1 School of Electrical and Computer Engineering, Pusan National University, Geumjeong-gu, Busan 46241, Korea; heeje@pusan.ac.kr (H.-J.K.); bjhgood84@naver.com (J.-H.B.)
2 Department of Energy Engineering, Inje University, 197 Inje-ro, Gimhae-si, Gyeongsangnamdo 50834, Korea; hwseo@inje.ac.kr
3 Department of Electronics, Kyushu University, 744 Motooka, Nishi-ku, Fukuoka 819-0395, Japan; siratani@ed.kyushu-u.ac.jp
* Correspondence: naga5673@gmail.com; Tel.: +82-10-4940-0437

Received: 5 July 2018; Accepted: 20 July 2018; Published: 24 July 2018


**Abstract:** Suppressing the charge recombination at the interface of photoanode/electrolyte is the crucial way to improve the quantum dot sensitized solar cells (QDSSCs) performance. In this scenario, ZnS/$SiO_2$ blocking layer was deposited on $TiO_2$/$CuInS_2$ QDs to inhibit the charge recombination at photoanode/electrolyte interface. As a result, the $TiO_2$/$CuInS_2$/ZnS/$SiO_2$ based QDSSCs delivers a power conversion efficiency (η) value of 4.63%, which is much higher than the $TiO_2$/$CuInS_2$ (2.15%) and $TiO_2$/$CuInS_2$/ZnS (3.23%) based QDSSCs. Impedance spectroscopy and open circuit voltage decay analyses indicate that ZnS/$SiO_2$ passivation layer on $TiO_2$/$CuInS_2$ suppress the charge recombination at the interface of photoanode/electrolyte and enhance the electron lifetime.

**Keywords:** QDSSCs; Charge recombination; ZnS/$SiO_2$; Passivation layer

## 1. Introduction

Semiconductor quantum dots (QDs) based on II-VI group such as CdSe [1], CdTe [2], CdS [3], PbS [4], PbSe [5], and etc. have been extensively studied for QD sensitized solar cell (QDSSC) and photocatalysis applications, due to tunable band gap, hot electron injection, higher absorption coefficients, and multiple excition generation (MEG) [6,7]. However, highly toxic Cd or Pb-containing QDs based solar cells show the excellent photostability and high power conversion efficiencies (PCEs). However, high toxicity of Cd or Pb still limit the commercial applications in consideration of environmental and health concerns. Therefore, the development of "green" QDs without carcinogenic heavy metal element is crucial for the practical utilizations of QDSSCs.

Less-toxic I−III−$VI_2$ group QDs, specifically $CuInS_2$ (CIS) QD has been attracted as "green" QDs due to high absorption coefficient (~$10^5$ $cm^{-1}$) and optimal band gap energy (1.0–1.5 eV), both of which make it a promising candidate as a sensitizer in QDSSCs [8–10]. There are two common approaches have been demonstrated for assembling $CuInS_2$ QDs onto $TiO_2$ electrodes: by direct adsorption or bifunctional-linker-assisted adsorption and by successive ionic layer adsorption [11,12]. Owing to its facile and reproducible preparation, the SILAR process gained much attention for depositing QDs onto $TiO_2$ surface with high QD loading and well controllable in size of QDs [13,14].

Chang et al. developed the $TiO_2$/$Cu_2S$/$CuInS_2$/ZnS photoanode using the SILAR process and achieved a PCE of 2.52% [15]. Zhou et al. prepared QDSSCs based on $CuInS_2$ and introduction of $In_2S_3$ buffer layer suing SILAR process, which presented as high as ~1.06% PCEs [16]. Meng et al. developed a $CuInS_2$ QDs on reduced graphene oxide sheets using facile one-pot solvothermal approach and

delivered a PCE of 1.5% [17]. Han et al. fabricated $PbS/CuInS_2/TiO_2$ using SILAR process and obtained a PCE of 4.11% [18]. However, the lower performance of QDSSC is due to severe charge recombination process at the $TiO_2$/QD/electrolyte interface. To reduce the charge recombination in QDSSCs, thin wide band gap inorganic barrier layer was deposited over $TiO_2$ electrode, which acts as an energy barrier hindering electrons from recombining. Until now, ZnS is a promising passivation layer for suppressing the interfacial recombination in QDSSCs [19]. The ZnS over layer is introduced by the facile SILAR process, which covers the $TiO_2$ layer and the surface of QDs toward the electrolyte. Therefore, the deposition of ZnS layer is useful technique to improve the solar cells performance due to the passivation of the QD surface states, yielding in suppression of the recombination processes [20].

Herein, $ZnS/SiO_2$ double barrier coating was sequentially deposited on $CuInS_2$ QD to suppress the recombination in QDSSCs. $TiO_2/CuInS_2/ZnS/SiO_2$ structure favors the improvement of photovoltaic properties of the QDSSCs. The QDSSC based on the $CuInS_2$ QD sensitizer and $ZnS/SiO_2$ double layer exhibits a PCE of 4.63% (with short circuit current density ($J_{SC}$) = 12.83 mA $cm^{-2}$, an open circuit voltage ($V_{OC}$) = 0.603 V, fill factor (FF) = 0.598) under AM 1.5 G one full sun illumination, which is much higher than the $CuInS_2$/ZnS (PCE = 3.23%) and $CuInS_2$ (PCE = 2.15%).

## 2. Results and Discussion

### *2.1. Morphological Characterization*

Figure 1(a,a1,b,b1,c,c1) show the scanning electron microscopy (SEM) images of the $CuInS_2$, $CuInS_2$/ZnS, and $CuInS_2/ZnS/SiO_2$ layers on the surface of $TiO_2$. The bare $CuInS_2$ film in Figure 1a,a1 exhibit uniformly distributed nanoparticles on the $TiO_2$ surface. All the samples exhibit the almost similar surface morphology and there is a slight increase in the particle size of with the deposition of ZnS and $ZnS/SiO_2$ layers; however, the specific change in size of particles is difficult to examine and was inconclusive. Therefore, elemental mapping from SEM analysis and X-ray photoelectron spectroscopy (XPS) measurements were conducted to identify the ZnS and $ZnS/SiO_2$ coatings on the surface of $TiO_2$. Moreover, the compositional distributions of a $TiO_2/CuInS_2/ZnS/SiO_2$ sample are further demonstrated by elemental mapping behavior, in which the homogeneous distribution and coexistence of Cu, In, Zn, S, Si and O elements are clearly observed in $TiO_2/CuInS_2/ZnS/SiO_2$ sample (Figure 2). Such elemental mapping results unambiguously indicate that the $CuInS_2$, ZnS and $SiO_2$ were deposited successfully on the $TiO_2$ surface.

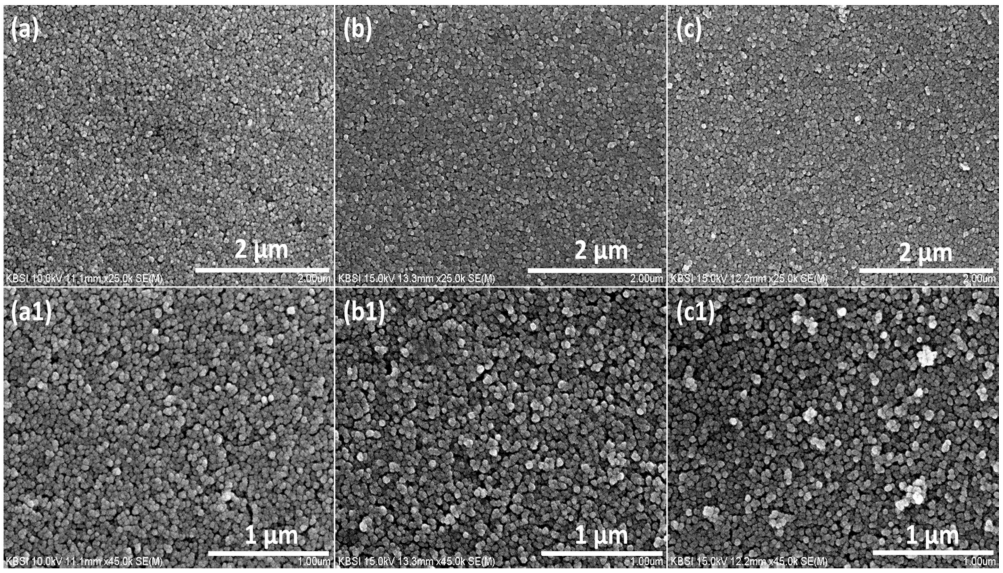


**Figure 1.** SEM images of the (**a**,**a**1) $CuInS_2$, (**b**,**b**1) $CuInS_2$/ZnS, and (**c**,**c**1) $CuInS_2/ZnS/SiO_2$ layers on the surface of $TiO_2$.

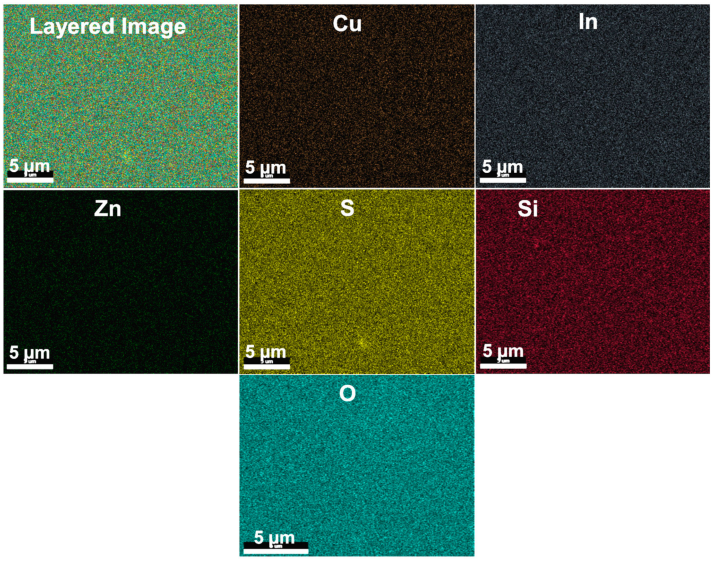


**Figure 2.** Elemental mapping images of the Cu, In, Zn, S, Si and O for the $TiO_2/CuInS_2/ZnS/SiO_2$ samples.

The composition of the $CuInS_2/ZnS/SiO_2$ sample was investigated by XPS, as depicted in Figure 3. The XPS survey spectra in Figure 3a depict peaks for $Ti_{2p}$, $O_{1s}$, $C_{1s}$, $Cu_{2p}$, $In_{3d}$, $Zn_{2p}$, $S_{2p}$, and $Si_{2p}$, respectively. The binding energy of Cu $2p_{3/2}$ and Cu $2p_{1/2}$ were observed at 932.9 and 952.7 eV, respectively (Figure 3b), with no evident shake-up satellite signals in this Cu2p spectrum. The two major peaks of In are observed at 445.4 eV and 452.9 eV for In $3d_{5/2}$ and In $3d_{3/2}$, respectively (Figure 3c). Figure 3d depicts the binding energies for Zn $2p_{3/2}$ and Zn $2p_{1/2}$ of the prepared sample of $CuInS_2/ZnS/SiO_2$ at 1023.2 eV and 1046.2 eV respectively. The S 2p spectrum was yielded peaks of S $2p_{3/2}$ and S $2p_{1/2}$ at 162.0 eV and 163.0 eV binding energies, respectively (Figure 3e). In the Si 2p spectrum (Figure 3f), the main peak observed at 103.2 eV has been ascribed to Si in the oxidized form ($SiO_2$) and the other shoulder peak can be assigned to the presence of crystalline Si (elemental Si).

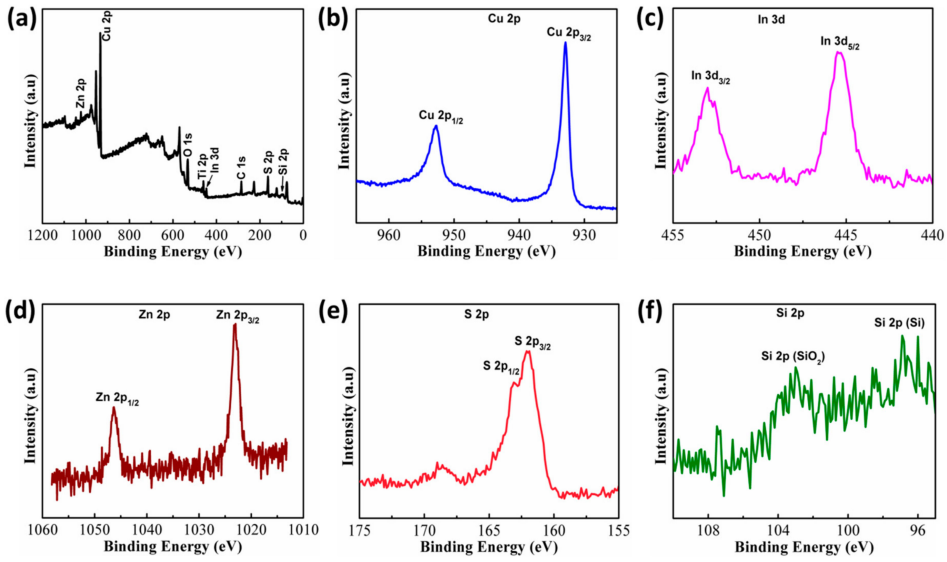


**Figure 3.** (**a**) XPS survey of $TiO_2/CuInS_2/ZnS/SiO_2$ film. Core-level XPS spectrum of (**b**) Cu 2p, (**c**) In 3d, (**d**) Zn 2p, (**e**) S 2p, and (**d**) Si 2p elements.

### 2.2. Electrochemical Characterization

The J-V curves of the QDSSCs based on various photoanodes were obtained under AM 1.5 illumination (100 mW $cm^{-2}$) are displayed in Figure 4 and the corresponding photovoltaic parameters are tabulated in Table 1. When only $CuInS_2$ are deposited on $TiO_2$ film, the QDSSC exhibits a $J_{SC}$ of 7.87 mA $cm^{-2}$, $V_{OC}$ of 0.509 V, FF of 0.537, resulting a low PCE of 2.15%. However, when ZnS and $ZnS/SiO_2$ passivation layers were deposited, all the photovoltaic parameters were greatly improved; the QDSSCs with a $ZnS/SiO_2$ layer exhibit the good performance, with $J_{SC}$, $V_{OC}$, and FF reaching 12.83 mA $cm^{-2}$, 0.603 V, and 0.598, respectively and the highest PCE of 4.63%, which is much higher than the PCE of 3.23% with a ZnS passivation layer. It is observed that the $ZnO/SiO_2$ layer exhibiting higher performance than the bare and ZnS layers in QDSSCs, which is due to suppression of recombination losses in QDSSCs and increases the charge collection efficiency.

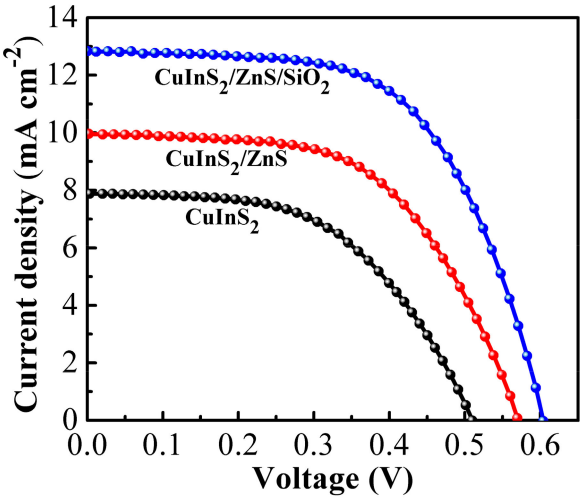


**Figure 4.** Current density−voltage (J−V) curves of $CuInS_2$, $CuInS_2/ZnS$ and $CuInS_2/ZnS/SiO_2$ based QDSSCs.

**Table 1.** Photovoltaic properties and EIS results of QDSSCs fabricated various sensitized conditions.

| Cell | $V_{oc}$ (V) | $J_{sc}$ (mA $cm^{-2}$) | FF | η% | $R_S$ (Ω) | $R_{CE}$ (Ω) | $R_{ct}$ (Ω) |
|---|---|---|---|---|---|---|---|
| $CuInS_2$ | 0.509 | 7.87 | 0.537 | 2.15 | 9.34 | 0.84 | 30.65 |
| $CuInS_2/ZnS$ | 0.569 | 9.95 | 0.571 | 3.23 | 10.03 | 1.03 | 23.95 |
| $CuInS_2/ZnS/SiO_2$ | 0.603 | 12.83 | 0.598 | 4.63 | 10.24 | 1.16 | 55.02 |

Electrochemical impedance spectroscopy (EIS) characterizations were conducted to identify the charge recombination processes in devices under forward bias ($V_{OC}$) and dark condition. Figure 5 depicts the EIS spectra of various photoelectrodes and the Nyquist plots were fitted using Z-view software with the equivalent circuit provided in the inset of Figure 5. The corresponding fitting results are shown in Table 1. The Nyquist plot consists of two semicircles and the first semicircle represents the resistance ($R_{CE}$) at the CE/electrolyte interface. The second semicircle denotes the charge transfer resistance ($R_{ct}$) at the interface of the $TiO_2$/QDs/electrolyte. At higher frequency, the intercept on the real axis corresponds to the series resistance ($R_s$) of FTO substrate and the resistance of FTO/$TiO_2$ [21,22]. It is noticed that there are no apparent differences observed in the $R_S$ and $R_{CE}$ due to the same CE and electrolyte used in these experiments. However, there is a noticeable difference in $R_{ct}$; the $R_{ct}$ value for the $CuInS_2/ZnS/SiO_2$ based QDSSCs is 55.02 Ω, while $R_{ct}$ value for the $CuInS_2/ZnS$ and $CuInS_2$ based QDSSCs are only 30.65 Ω and 23.95 Ω, respectively. The charge recombination resistance at the $TiO_2$/QDs/electrolyte interface is mainly observed by $R_{ct}$. The higher $R_{ct}$ value represents the suppressed recombination of the electrons and holes, and enhances the

electron transfer process at the interface of $TiO_2$/QDs/electrolyte. Therefore, it is confirmed that the deposition of $ZnS/SiO_2$ layer on the $CuInS_2$ QDs favors the efficient electron transfer from $CuinS_2$ to $TiO_2$ photoanodes with suppression of the interfacial charge recombination processes, which is more effectively than that of the ZnS passivation layer.

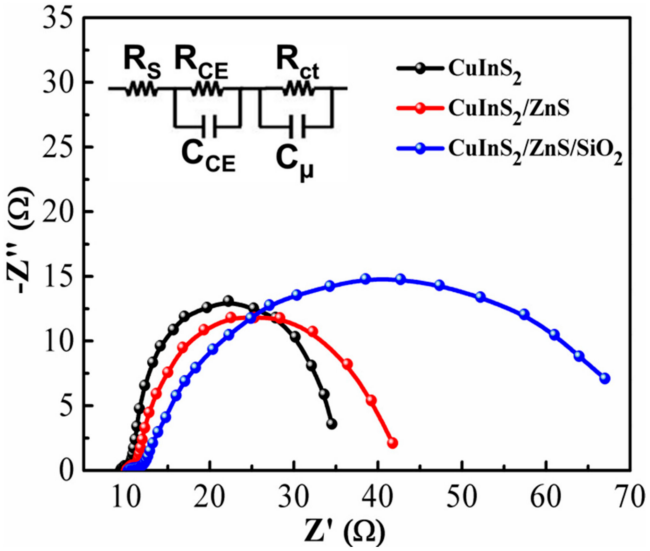


**Figure 5.** EIS curves of QDSSCs based $CuInS_2$ and $CuInS_2$/ZnS and $CuInS_2/ZnS/SiO_2$ cells in the form of Nyquist-plots and the inset shows the equivalent circuit used to fit the impedance spectra.

Furthermore, Open circuit voltage decay (OCVD) measurements were carried out to study the charge recombination process in QDSSCs and the results. OCVD analysis of QDSSCs was performed during relaxation form an illuminated quasiequilibrium state to the darkness. Figure 6 depicts the OCVD plots of the QDSSCs based on $CuInS_2$, $CuInS_2$/ZnS and $CuInS_2/ZnS/SiO_2$ photoanodes. Apparently, the $CuInS_2/ZnS/SiO_2$ cell delivered considerably longer decay times than the $CuInS_2$ and $CuInS_2$/ZnS cells, indicating a suppression of charge recombination process. Moreover, the $V_{OC}$ decay and electron life time are directly related according to following equation [23]:

$$\tau_e = -\left(\frac{k_B T}{e}\right)\left(\frac{dV_{OC}}{dt}\right)^{-1} \quad (1)$$

where $k_B$ is the Boltzmann constant, $T$ is the absolute temperature, and $e$ is the electronic charge. It can be noticed that the $\tau_e$ of all the devices increases with decreasing $V_{OC}$. Among the QDSSCs investigated, the $CuInS_2/ZnS/SiO_2$ delivers longer $\tau_e$ than the $CuInS_2$/ZnS and $CuInS_2$ devices, implying suppressed recombination and efficient electron transfer at the $TiO_2$/QDs/electrolyte, which is consistent with EIS analysis. Therefore, the slower $V_{OC}$ decay and longer $\tau_e$ of the $CuInS_2/ZnS/SiO_2$ device efficiently suppressed the electron recombination from $TiO_2$ and QDs to electrolyte and higher charge collection efficiency contribute to the increased photovoltaic performance.

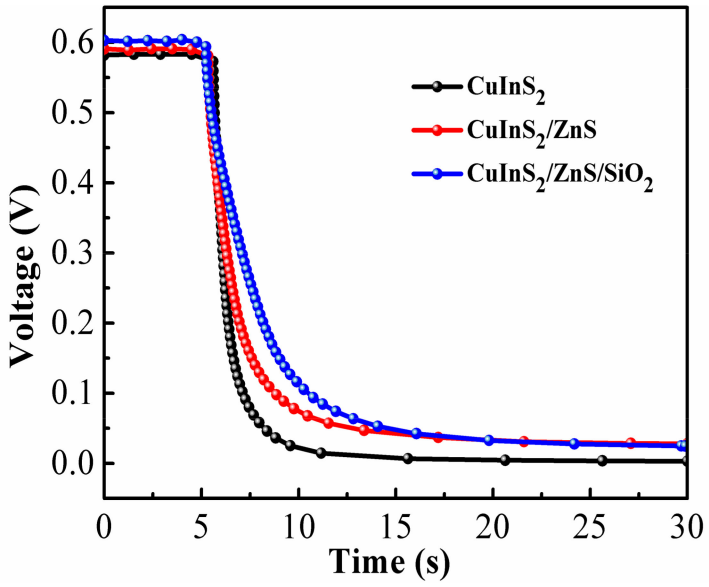


**Figure 6.** OCVD curves of QDSSCs based $CuInS_2$ and $CuInS_2/ZnS$ and $CuInS_2/ZnS/SiO_2$ cells.

Several paths for charge recombination occur at the $TiO_2$/QDs/electrolyte interface, which suppress the performance of QDSSCs. The deposition of $ZnS/SiO_2$ layer on the surface of $TiO_2/CuInS_2$ can effectively suppress the charge recombination process at the photoanode/electrolyte interface (Figure 7) and enhance the QDSSCs performance.

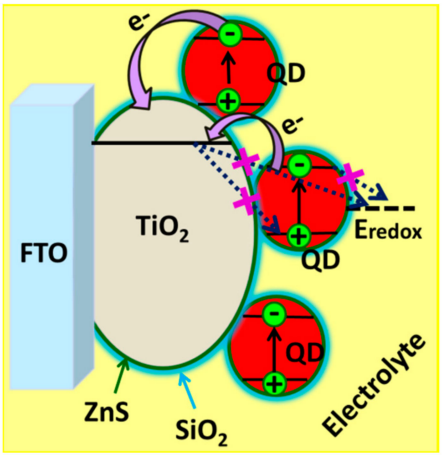


**Figure 7.** Possible charge transfer behavior in the $TiO_2/CuInS_2/ZnS/SiO_2$ QDSSCs.

## 3. Materials and Methods

### *3.1. Preparation of $TiO_2$ Electrodes*

$TiO_2$ paste (20 nm, Ti-Nanoxide HT/TP, Solaronix) was doctor bladed on fluorine-doped tin oxide (FTO, 1.3 × 1.6 $cm^2$) substrate and heated at 450 °C for 30 min. The film thickness was about 7.5 μm with an active area of 0.25 $cm^2$ [24].

### *3.2. Deposition of $CuInS_2$ QDs on $TiO_2$ Electrodes*

$CuInS_2$ QDs was deposited on the $TiO_2$ substrate using the SILAR process. $TiO_2$ electrodes were immersed into the three different solutions: one of 0.05 M of $Cu(NO_3)_2$ for 2 min, another of 0.05 M of $In(NO_3)_3$ for 2 min, and a final one of 0.1 M of $Na_2S$ for 5 min. Following each immersion, the samples

were rinsed with deionized (DI) water for 1 min to remove the excess precursors. This procedure comprises one $CuInS_2$ SILAR cycle and was repeated six times.

### *3.3. Deposition of ZnS, ZnS/SiO$_2$ Passivation Layers on TiO$_2$/CuInS$_2$ Electrodes*

The ZnS passivation layer was deposited on $TiO_2/CuInS_2$ electrodes by a SILAR process. Typically, $TiO_2/CuInS_2$ electrodes were successively immersed into aqueous solutions containing 0.1 M of $Zn(NO_3)_2$ and 0.1 M $Na_2S$ for 1 min, respectively. This process was repeated for three times and the electrode is named as $CuInS_2/ZnS$. Furthermore, $SiO_2$ coating was deposited by dipping the $CuInS_2/ZnS$ electrodes in ethanol solution containing 0.01 M tetraethylorthosilicate and 0.1 M $NH_4OH$ for 1 h. The as-fabricated electrode is termed as $CuInS_2/ZnS/SiO_2$.

### *3.4. QDSSC Fabrication*

CuS CE on FTO substrate was fabricated according to the literature [25]. The photoanode and CuS CEs were combined using sealant (SX 1170-60, Solaronix) and the space between the electrodes was filled with polysulfide electrolyte (1 M $Na_2S$, 2 M S, and 0.2 M KCl in methanol and water at a ratio of 7:3).

### *3.5. Characterizations*

The morphology of the samples were evaluated by SEM (S-2400, Hitachi). XPS measurement was investigated using VG Scientific ESCALAB 250. The J-V measurements were examined under AM 1.5 sunglight (100 mW $cm^{-2}$) using an ABET Technologies (USA) solar simulator. EIS was investigated using a BioLogic SP-150 work station under one sun illumination over the frequency of 100 mHz–500 kHz.

## 4. Conclusions

Introduction of $ZnS/SiO_2$ passivation layer on $TiO_2/CuInS_2$ QDs has been demonstrated to be an effective and promising approach to significantly suppress the charge recombination at the interface of photoanode/electrolyte and enhance the power conversion efficiency. Interestingly, an overall $\eta$ of 4.63% was obtained for the $TiO_2/CuInS_2/ZnS/SiO_2$ device, which is 43% enhancement over the $\eta$ = 3.23% for the $TiO_2/CuInS_2/ZnS$ and more than 115% increment over the $\eta$ = 2.15% for the $TiO_2/CuInS_2$ device. Overall, $ZnS/SiO_2$ passivation layer is an effective approach to enhance the overall power conversion efficiency of QDSSCs.

**Author Contributions:** H.J.K. and J.H.B performed device performance measurements. H.S. and M.S. helped in the analysis of the data. C.V.V.M.G. designed this research idea and writing the manuscript.

**Funding:** This research was supported by Basic Science Research Program through the National Research Foundation of Korea (NRF) funded by the Ministry of Education, ICT and Future planning (NRF-2016K2A9A2A08003717).

**Conflicts of Interest:** The authors declare no conflict of interest.

## References

1. Lee, H.J.; Wang, M.; Chen, P.; Gamelin, D.R.; Zakeeruddin, S.M.; Grätzel, M.; Nazeeruddin, M.K. Efficient CdSe Quantum Dot-Sensitized Solar Cells Prepared by an Improved Successive Ionic Layer Adsorption and Reaction Process. *Nano Lett.* **2009**, *9*, 4221–4227. [CrossRef] [PubMed]
2. Shen, X.; Jia, J.; Lin, Y.; Zhou, X. Enhanced performance of CdTe quantum dot sensitized solar cell via anion exchanges. *J. Power Sources* **2015**, *277*, 215–221. [CrossRef]
3. Gopi, C.V.V.M.; Haritha, M.V.; Kim, S.K.; Kim, H.J. A strategy to improve the energy conversion efficiency and stability of quantum dot-sensitized solar cells using manganese-doped cadmium sulfide quantum dots. *Dalton Trans.* **2015**, *44*, 630–638. [CrossRef] [PubMed]

4. González-Pedro, V.; Sima, C.; Marzari, G.; Boix, P.P.; Giménez, S.; Shen, Q.; Dittrich, T.; Seró, I.M. High performance PbS Quantum Dot Sensitized Solar Cells exceeding 4% efficiency: the role of metal precursors in the electron injection and charge separation. *Phys. Chem. Chem. Phys.* **2013**, *15*, 13835–13843. [CrossRef] [PubMed]
5. Zhang, J.; Gao, J.; Church, C.P.; Miller, E.M.; Luther, J.M.; Klimov, V.I.; Beard, M.C. PbSe Quantum Dot Solar Cells with More than 6% Efficiency Fabricated in Ambient Atmosphere. *Nano Lett.* **2014**, *14*, 6010–6015. [CrossRef] [PubMed]
6. Kamat, P.V. Quantum Dot Solar Cells. Semiconductor Nanocrystals as Light Harvesters. *J. Phys. Chem. C* **2008**, *112*, 18737–18753. [CrossRef]
7. Kongkanand, A.; Tvrdy, K.; Takechi, K.; Kuno, M.; Kamat, P.V. Quantum Dot Solar Cells. Tuning Photoresponse through Size and Shape Control of CdSe−$TiO_2$ Architecture. *J. Am. Chem. Soc.* **2008**, *130*, 4007–4015. [CrossRef] [PubMed]
8. Booth, M.; Brown, A.P.; Evans, S.D.; Critchley, K. Determining the Concentration of $CuInS_2$ Quantum Dots from the Size-Dependent Molar Extinction Coefficient. *Chem. Mater.* **2012**, *24*, 2064–2070. [CrossRef]
9. Leach, A.D.P.; Macdonald, J.E. Optoelectronic Properties of $CuInS_2$ Nanocrystals and Their Origin. *J. Phys. Chem. Lett.* **2016**, *7*, 572–583. [CrossRef] [PubMed]
10. Li, T.L.; Lee, Y.L.; Teng, H. $CuInS_2$ quantum dots coated with CdS as high-performance sensitizers for $TiO_2$ electrodes in photoelectrochemical cells. *J. Mater. Chem.* **2011**, *21*, 5089–5098. [CrossRef]
11. Bang, J.H.; Kamat, P.V. Quantum Dot Sensitized Solar Cells. A Tale of Two Semiconductor Nanocrystals: CdSe and CdTe. *ACS Nano* **2009**, *3*, 1467–1476. [CrossRef] [PubMed]
12. Xu, X.; Wan, Q.; Luan, C.; Mei, F.; Zhao, Q.; An, P.; Liang, Z.; Xu, G.; Zapien, J.A. Fabrication of CuInS2-Sensitized Solar Cells via an Improved SILAR Process and Its Interface Electron Recombination. *ACS Appl. Mater. Interfaces* **2013**, *5*, 10605–10613. [CrossRef] [PubMed]
13. Kontos, A.G.; Likodimos, V.; Vassalou, E.; Kapogianni, I.; Raptis, Y.S.; Raptis, C.; Falaras, P. Nanostructured titania films sensitized by quantum dot chalcogenides. *Nanoscale Res. Lett.* **2011**, *6*, 266–271. [CrossRef] [PubMed]
14. Lee, H.J.; Bang, J.; Park, J.; Kim, S.; Park, S.M. Multilayered semiconductor (CdS/CdSe/ZnS)-sensitized $TiO_2$ mesoporous solar cells: All prepared by successive ionic layer adsorption and reaction processes. *Chem. Mater.* **2010**, *22*, 5636–5643. [CrossRef]
15. Chang, J.Y.; Su, L.F.; Li, C.H.; Chang, C.C.; Lin, J.M. Efficient "green" quantum dot-sensitized solar cells based on $Cu_2S$–$CuInS_2$–ZnSe architecture. *Chem. Commun.* **2012**, *48*, 4848–4850. [CrossRef] [PubMed]
16. Zhou, Z.; Yuan, S.; Fan, J.; Hou, Z.; Zhou, W.; Du, Z.; Wu, S. $CuInS_2$ quantum dot-sensitized $TiO_2$ nanorod array photoelectrodes: Synthesis and performance optimization. *Nanoscale Res. Lett.* **2012**, *7*, 652–659. [CrossRef] [PubMed]
17. Meng, W.; Zhou, X.; Qiu, Z.; Liu, C.; Chen, J.; Yue, W.; Wang, M.; Bi, H. Reduced graphene oxide-supported aggregates of $CuInS_2$ quantum dots as an effective hybrid electron acceptor for polymer-based solar cells. *Carbon* **2016**, *96*, 532–540. [CrossRef]
18. Han, M.; Jia, J.; Yu, L.; Yi, G. Fabrication and photoelectrochemical characteristics of $CuInS_2$ and PbS quantum dot co-sensitized $TiO_2$ nanorod photoelectrodes. *RSC Adv.* **2015**, *5*, 51493–51500. [CrossRef]
19. Diguna, L.J.; Qing, S.; Kobayashi, J.; Toyoda, T. High efficiency of CdSe quantum-dot-sensitized $TiO_2$ inverse opal solar cells. *Appl. Phys. Lett.* **2007**, *91*, 023116–023118. [CrossRef]
20. De la Fuente, M.S.; Sánchez, R.S.; González-Pedro, V.; Boix, P.P.; Mhaisalkar, S.G.; Rincón, M.E.; Bisquert, J.; Mora-Seró, I. Effect of Organic and Inorganic Passivation in Quantum-Dot-Sensitized Solar Cells. *J. Phys. Chem. Lett.* **2013**, *4*, 1519–1525. [CrossRef] [PubMed]
21. Gopi, C.V.V.M.; Haritha, M.V.; Kim, S.K.; Kim, H.J. Improved photovoltaic performance and stability of quantum dot sensitized solar cells using Mn–ZnSe shell structure with enhanced light absorption and recombination control. *Nanoscale* **2015**, *7*, 12552–12563. [CrossRef] [PubMed]
22. Kim, H.J.; Kim, S.W.; Gopi, C.V.V.M.; Kim, S.K.; Rao, S.S.; Jeong, M.S. Improved performance of quantum dot-sensitized solar cells adopting a highly efficient cobalt sulfide/nickel sulfide composite thin film counter electrode. *J. Power Sources* **2014**, *268*, 163–170. [CrossRef]
23. Liu, Z.; Miyauchi, M.; Uemura, Y.; Cui, Y.; Hara, K.; Zhao, Z.; Sunahara, K.; Furube, A. Enhancing the performance of quantum dots sensitized solar cell by $SiO_2$ surface coating. *Appl. Phys. Lett.* **2010**, *96*. [CrossRef]

24. Kim, H.J.; Kim, D.J.; Rao, S.S.; Savariraj, A.D.; Kyoung, K.S.; Son, M.K.; Gopi, C.V.V.M.; Prabakar, K. Highly efficient solution processed nanorice structured NiS counterelectrode for quantum dot sensitized solar cell. *Electrochim. Acta* **2014**, *127*, 427–432. [CrossRef]
25. Kim, H.J.; Sik, L.M.; Gopi, C.V.V.M.; Haritha, M.V.; Rao, S.S.; Kim, S.K. Cost-effective and morphology controllable PVP based highly efficient CuS counter electrodes for high-efficiency quantum dot-sensitized solar cells. *Dalton Trans.* **2015**, *44*, 11340–11351. [CrossRef] [PubMed]